RNPS No. 2142
ISSN 2072-6287
Versión Digital

CENATAV
Centro de Aplicaciones de Tecnologías de Avanzada
MINISTERIO DE LA INDUSTRIA BÁSICA

REPORTE TÉCNICO
Reconocimiento de Patrones

SERIE AZUL

Image Processing Methods for X-Ray Luggage Images: A Survey

Alexey Guilarte Noa and
Edel B. García Reyes

RT_043 **octubre 2011**

7ma. No. 21812 e/218 y 222,
Rpto. Siboney, Playa;
La Habana.
Cuba. C.P. 12200
www.cenatav.co.cu

RNPS No. 2142
ISSN 2072-6287
Versión Digital

SERIE AZUL

CENATAV
Centro de Aplicaciones de Tecnologías de Avanzada
MINISTERIO DE LA INDUSTRIA BÁSICA

REPORTE TÉCNICO
Reconocimiento de Patrones

Image Processing Methods for X-Ray Luggage Images: A Survey

Alexey Guilarte Noa and
Edel B. García Reyes

RT_043 **octubre 2011**

7ma. No. 21812 e/218 y 222,
Rpto. Siboney, Playa;
La Habana.
Cuba. C.P. 12200
www.cenatav.co.cu

Image Processing Methods for X-Ray Luggage Images: A Survey

Alexey Guilarte Noa and Edel B. García Reyes

Pattern Recognition Department,
Advanced Technologies Application Center (CENATAV),
Havana, Cuba
{aguilarte,egarcia}@cenatav.co.cu

RT_043, Serie Azul, CENATAV
Aceptado: 4 de octubre de 2011

Abstract. The detection of threatening objects using x-ray luggage scan images has become an important means of aviation security nowadays. Although tremendous amount of efforts have been focused on automatic detection of objects for medical systems, security applications were not at the forefront of research until the events of September 11th and most airport screening is still based on the manual detection of potential threat objects by human experts. A variety of so-called “image enhancements” functions to help decision making by humans is now a recognized area of critical need. In this technical report we present the state of the art about image enhancement methods for single and dual energy x-ray images, we propose a new taxonomy, grouping the different approaches and stressing their limitations as a starting point to future contributions in this field.

Keywords: x-ray, image enhancement, threat objects.

Resumen. La detección de objetos amenazantes utilizando imágenes de rayos X de escáner de equipaje se ha convertido en un importante medio de seguridad de la aviación en la actualidad. A pesar de la gran cantidad de esfuerzos que se han centrado en la detección automática de objetos para sistemas médicos, las aplicaciones de seguridad no estuvieron en la vanguardia de la investigación hasta los acontecimientos del 11 de septiembre y el control en los aeropuertos se sigue basando mayormente en la detección manual de objetos de amenaza potencial, por los expertos humanos. Una variedad de las funciones llamadas "mejoras de imagen" es ahora una zona reconocida de necesidad crítica para ayudar a la toma de decisiones por los seres humanos. En este informe técnico se presenta el estado del arte de los métodos de mejora de la imagen de rayos X de simple y doble energía, se propone una nueva taxonomía, se agrupan los distintos enfoques y se destacan sus limitaciones como punto de partida para futuras contribuciones en este campo.

Palabras clave: rayos x, mejora de imagen, objetos amenazantes.

1 Introduction

In a world threatened by terrorism, x-ray luggage inspection systems play an important role in ensuring air travelers security (see, Figure 1). X-rays have been used for several years in airport screening task and a number of techniques based on x-rays have been employed for detecting weapons and explosives. Among the most popular methods are conventional transmission imaging and dual energy x-ray imaging [1].

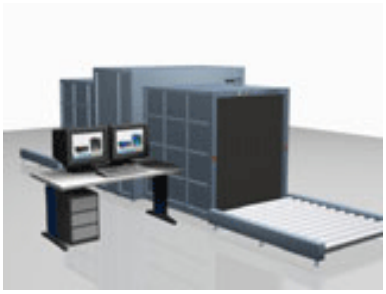

Fig. 1. X-ray luggage inspection systems.

Conventional x-ray systems are effective in detecting objects of metallic composition (knives and guns), while low-density weapons could easily go unchecked. Objects such as metallic guns and knives, which are characterized by high-density responses in x-ray images, are also easily spotted by screeners. However, objects like plastic, glass, and wooden sharp items are characterized by very faint, low-density responses in x-ray projections and are very hard to distinguish by screeners. The principal limitation of these devices is that they cannot distinguish between a thin sheet of strong absorber and a thick slab of weak absorber. Figure 2 depicts a conventional x-ray image.

Fig. 2. Conventional x-ray image.

Dual energy x-ray systems (see, Figure 3) are used to identify materials in luggage by comparing two images of the luggage obtained at two different x-ray energy levels (high energy and low energy). When high-energy x-rays penetrate objects, the energy absorption depends primarily on the material's density. The higher the density is, the higher the energy absorption by the object, and hence the darker the image. For low-energy x-rays, however, the energy absorption depends primarily on the effective atomic number of the material as well as the thickness of the object. Therefore, areas of high density materials such as metal are dark in both low and high-energy x-ray images, but areas of lighter elements are shown as darker regions in low-energy images compared to high-energy images. Commercial dual energy systems use the information from the two images to estimate the atomic number of the materials. Theoretically, an object's material type can be uniquely determined using its density and atomic number, however these devices provide poor information about the density of the objects and only an estimate of atomic number can be generated, the effective atomic number which represents the atomic number of all object crossed by the x-ray photon. As a result of these limitations, the false alarm rate of dual energy x-ray luggage detection systems reaches roughly 30% [1]. According to Federal Aviation Agency (FAA) an acceptable false alarm rate is less than 5 percent.

The inspection task in most airports of the world is still based on the manual detection of potential threatening objects by human experts; due to this, security training is relying heavily on the object recognition test (ORT) as a means of qualifying human airport luggage screeners [2] and a variety of

so-called “image enhancements” functions to aid decision making by humans is now a recognized area of critical need. A study of the effect of image enhancement functions on x-ray detection performance is available on [3].The main objective of such image enhancements functions is to process an image so that the result is more suitable than the original image for a specific application as for example x-ray screening at airports [4]. In x-ray images, the image enhancements might increase the visibility of objects within the bag and remove background noise.

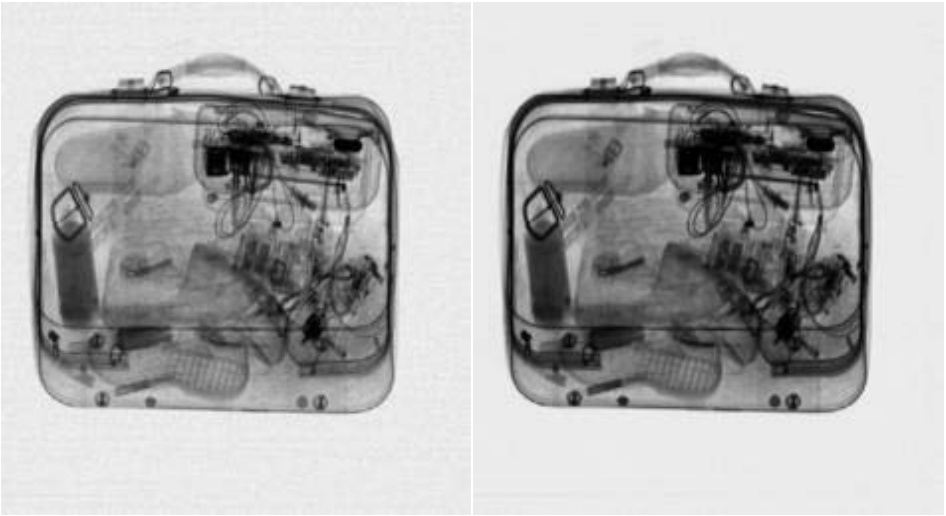

Fig. 3. Two x-ray images of a dual energy X-ray system. High energy x-ray image *(left) and* low energy x-ray images *(right).*

In the literature there are several methods that have made progress in processing x-ray luggage images. The methods can be clustered into two primary groups: those designed for single conventional x-ray image and those that used information of two images obtained at two different x-ray energy levels (dual energy x-ray systems) to obtain a fuse image.

The methods of the first group improve the image quality using traditional techniques like image enhancement, declustering and pseudo-coloring algorithms. Nercessian et al. [5] proposed an image enhancement via logarithmic transform histogram shifting (LTHS). The method enhances an image by first taking its discrete cosine transform (DCT) and transforming the DCT magnitude coefficients into the logarithm domain. The enhanced image is obtained via the inverse discrete cosine transform (IDCT). Methods such as contrast stretching, gamma intensity correction, logarithmic intensity adjustment and histogram equalization have become popular methods for image enhancement and were applied in [6] [7] by Abidi et al. to raw x-ray data of luggage scenes containing low density threat items. They combined these methods with declustering techniques and obtained a significant increase of up to 62%, as compared to the original image, in the rate of threat detection. The goal of the hashing algorithmic is to progressively decluster an image scene and produce separate image objects of different intensity values. This process should ease the screener’s task by making the threat more visible and reducing interference of harmless items with the inspection process. Since it is known that human beings can only discern a few dozen gray level values while they can distinguish thousands of colors a series of linear and nonlinear pseudo-coloring maps were designed in [8] and applied to single energy x-ray luggage scans to assist airport screeners in identifying and detecting threat items. According to the authors, the use of color for human interpretation could only improve the number of objects that can be distinguished. A significant increase of up to 97% was reported compared to results from the original data in the rate of threat detection.

The two images based on methods are focused in combining information from the low energy x-ray image and the high-energy x-ray image such that the produced combined image is more amenable for a successful screeners’ interpretation. Commercial dual-energy x-ray luggage inspection systems feature

dual-energy analysis to estimate the atomic number of materials in luggage fusing the information of images at low-energy and a high-energy. Generally the fuse image is a colored image where the red shades represent organic material, blue shades represent inorganic material and the green shades represent a mixture between inorganic and organic. Zheng [9] described a dual energy x-ray image fusion method using spatial information. The method first classifies each pixel in a luggage scene into either background pixel or detail pixel, and then highlights detail pixels with the assumption that detail pixels carry the features of interest in the luggage scene. Zhiyu Chen, et al, [10] developed a combinational approach based on the wavelet transform. The method first transforms each image into corresponding wavelet coefficient images using the discrete wavelet transform (DWT). Then, following a fusion rule, the fused wavelet coefficients are computed from the wavelet coefficients of the source images. The inverse DWT (IDWT) is then applied to the fused wavelet coefficients to obtain the fused image. Since background noise often gets amplified during the fusion process the authors apply a background-subtraction-based noise reduction technique. The de-noised image is then processed using an enhancement technique based on histogram to reconstruct the final image.

Most of these x-ray image analysis methods use algorithms that were developed for visible spectrum images. These methods assume that objects are opaque and occlude each other. X-ray photons, however, penetrate most materials. As a result, all objects along an x-ray path attenuate the x-ray and contribute to the final measured intensity. This is what allows x-ray imaging to “see through” objects [11].

In this technical report we make an analysis of the different methods and stress their limitations as a starting point to future contributions in the field. The rest of the report is organized as follows. Chapter 2 presents the state of the arts in x-ray carry-on luggage inspection systems, gray scale image enhancement, image segmentation and pseudo coloring. Image fusion techniques are introduced in Chapter 3.Chapter 4 presents the new taxonomy proposed.

2 Improved Image Quality in Single X-ray Images

There are some methods published that have tried to improve image quality on single x-ray images and they have proved very useful to improve the rate of detection of threatening objects in x-ray images scans. These methods can be grouped into three main categories. Methods for image enhancement, declustering or hashing methods and methods based on false color schemes. Often these approaches are combined for better results. These methods will be described in this chapter.

2.1 Image Enhancement Methods

Although the primary goal of image enhancement is generally to provide a clearer image to the human eye, it is used in the automatic object detection problem as a preprocessing step to provide more accurate segmentation or more accurate edge maps. There are several methods that have been proved useful to improve the image quality in x-ray images; among the most popular are contrast stretching, gamma intensity correction, logarithmic intensity correction, standard measure techniques and histogram equalization [6][7]. Recently, Silver et al. (Shahan Nercessian K. P., 2008) presented an enhancement technique based upon a new application of histograms on transform domain coefficients called logarithmic transform coefficient histogram shifting (LTHS).

2.1.1 Linear Contrast Stretching

This procedure stretching the pixels value range within a given image so that the pixels value cover a wider range or entire range (for example in a 8 bit gray-scale image, the entire pixel values l range is 0 to 255). Linear contrast enhancement can be mathematically formulated by:

$$G(x,y) = a \times f(x,y) + b$$

Where $f(x, y)$ is the value of the original image at pixel location (*x,y)*, and *G*(*x,y*) is the resulting enhanced image value at the same location; *a* and *b* are coefficients to be computed according to the desired range of the output images. Figure 4 shows the result of an example of linear contrast stretching operation.

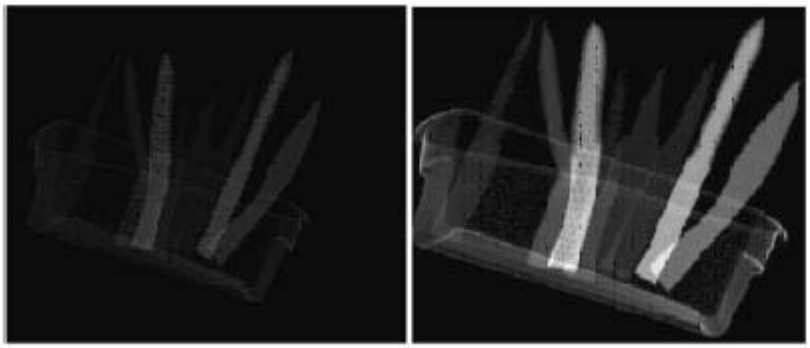

Fig. 4. Original image *(left)* and the image after linear contrast stretching process *(right)*. Tomado de [7].

2.1.2 Gamma Intensity Correction

Gamma intensity correction procedure modifies the pixels value based on the equation:

$$I' = c\, I^{\gamma}$$

Where *I* and *I'* are the original and enhanced images and *c* is a scaling factor. Gamma values (γ) lesser than 1 emphasize light areas and values greater than 1 emphasize dark areas of the original image after the conversion is performed. Figure 5 shows the result of gamma intensity correction method for several values of gamma.

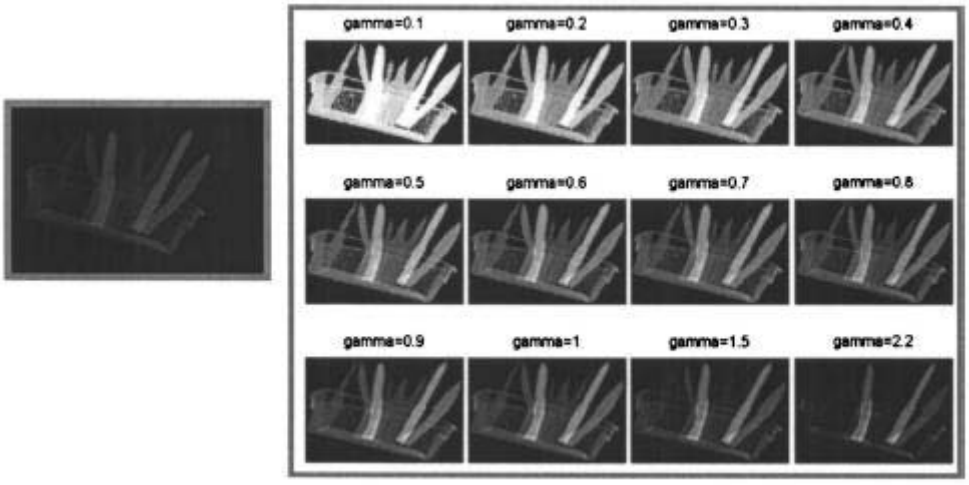

Fig. 5. Original image *(left)* and the image after gamma correction for several values of gamma *(right)*. Tomado de [7].

2.1.3 Logarithmic Intensity Correction

Logarithmic intensity adjustment can take several forms but typically might be expressed as:

$$I' = s \times \ln(I + 1)$$

Where *I'* and *I* are the output and input gray-scale images, and *s* is a scaling factor. Figure 6 shows the result of logarithmic intensity correction method.

Fig. 6. Original image *(left)* and the image after logarithmic correction *(right)*. Tomado de [7].

2.1.4 Standard Measure Technique

The standard measure is expressed by:

$$I' = \frac{I - \overline{I_s}}{\sigma_s}$$

where I is the gray level value of a pixel (x, y) in the original image, $\overline{I_s}$ is the mean gray value in a neighborhood s of image I around pixel (x, y), σ_s is the standard deviation of s, and I' is the output value at pixel (x, y). After the initial values are computed, the resulting image is obtained by linearly scaling initial results to be between 0 and 255. This accounts for potential negative values. Fig. 7 shows the result of the standard measure method.

Fig. 7. Original image *(left)* and the image after applied standard measure technique *(right)*. Tomado de [7].

2.1.5 Histogram Equalization

This image enhancement technique is based on the alteration of the image histogram characteristics to provide as close to a uniform distribution as possible. Figure 8 shows the result of histogram equalization.

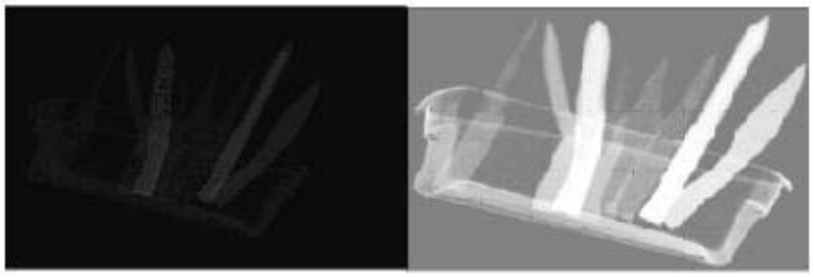

Fig. 8. Original image *(left)* and the image after histogram equalization *(right)*. Tomado de [7].

2.1.6 Logarithmic Transform Coefficient Histogram Shifting

Logarithmic Transform Histogram Shifting [12] enhances an image by first taking its DCT and transforming the DCT magnitude coefficients into the logarithm domain using:

$$\bar{X}(i,j) = \log\Big(|X(i,j)| + \lambda\Big)$$

where λ is a shifting coefficient. A coefficient histogram is calculated and shifted by k bins. Transform data is mapped to the shifted histogram and the data is exponentiated. Lastly, phase is restored and the inverse DCT of the transform data is taken to return to the spatial domain (see Figure 9). The algorithm uses a measure of enhancement by entropy to choose the optimal value of k. This method was used by Panetta et al. [5] and proved to be useful to enhancement x-ray images (see Figure 10).

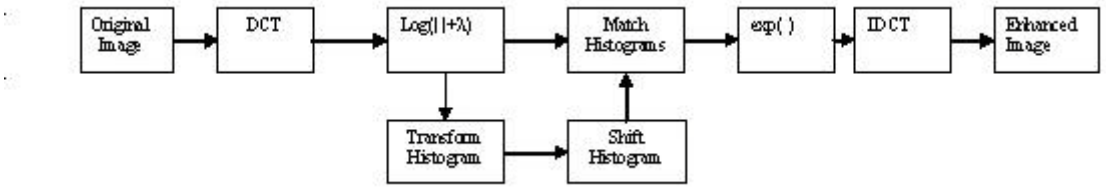

Fig. 9. Block Diagram of Logarithmic Transform Histogram Shifting.

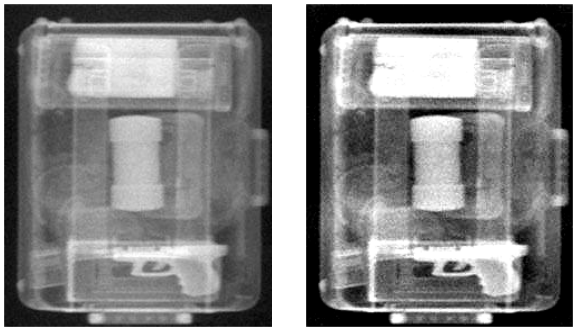

(a) (b)

Fig. 10. (a) Original image and (b) enhanced image using LTHS.

2.2 Hashing Methods

The goal of these techniques is declustering or hashing an image scene, producing separate image slices objects of different intensity values making the threats more visible and reducing interference of harmless items with the inspection process. In the published works [6][7] the image hashing is performed via intensity slicing and involves selecting some portion of the range of pixel values of an original image and producing an image slice containing only the selected portion of that pixel range. These methods do not address the transparency present in the x-ray images where the objects are mixed, but as a result of the separation, regions are obtained where the intensity is homogeneous and not the objects that make up the mixes.

2.2.1 Equal Interval Image Slicing

This is the simplest procedure and consists in slicing the image in equal width slices covering the entire dynamic range of the image. Figure 11 (a) depicts three equal slices representation for a 16 bit gray-scale image.

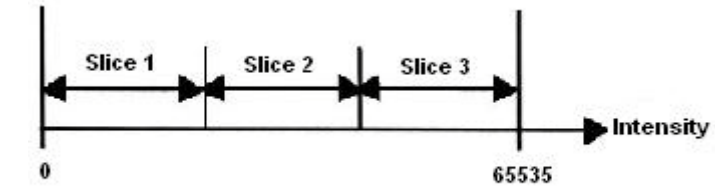

(a)

(b)

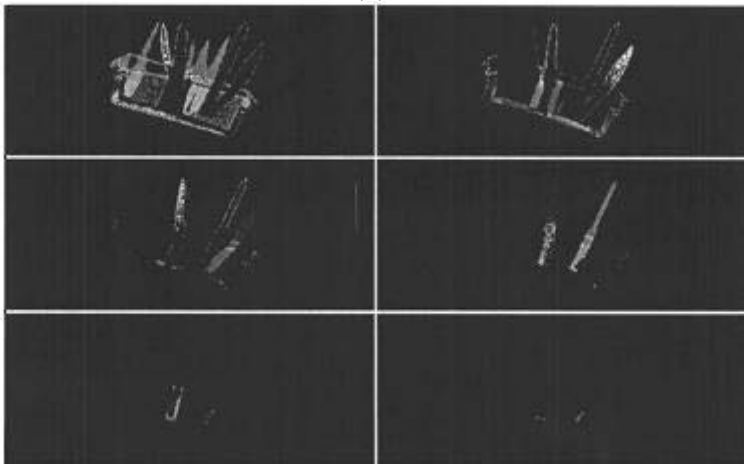

(c)

Fig. 11. (a) depicts three-slice equal interval representation, (b) original image and (c) six-slice equal interval hashing applied to (b). Tomado de [7].

2.2.2 Cumulative Image Slicing

This method is similar to equal interval slicing; the difference here is that the slices are cumulative. For example, if the original image is divided into six sub-images, the first image slice shows all pixels in sub-image 1, the second slice all pixels in sub-images 1 and 2, and so on .The last slice shows the original image. Figure 12 (b) shows six-slice cumulative hashing applied to figure 12 (a)

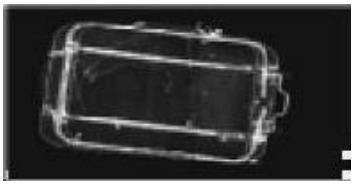

(a)

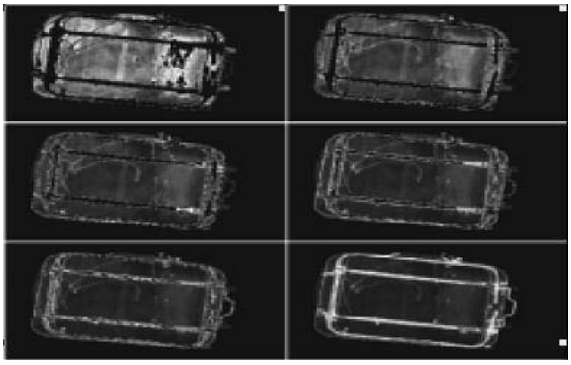

(b)

Fig. 12. (a) Original image and (b) six-slice cumulative hashing applied to (a). Tomado de [7].

2.2.3 Image Slicing with H Domes

Slicing with H domes is slightly different to equal and cumulative image slicing. The original image is used as a mask and markers are obtained subtracting a fixed value H to the mask (see Figure 13). The mask is morphologically reconstructed using the marker and the reconstructed image is subtracted from the mask providing H domes of the original image. Varying the H value we can obtain several image slices. Figure 14 show the result obtained for a specific H.

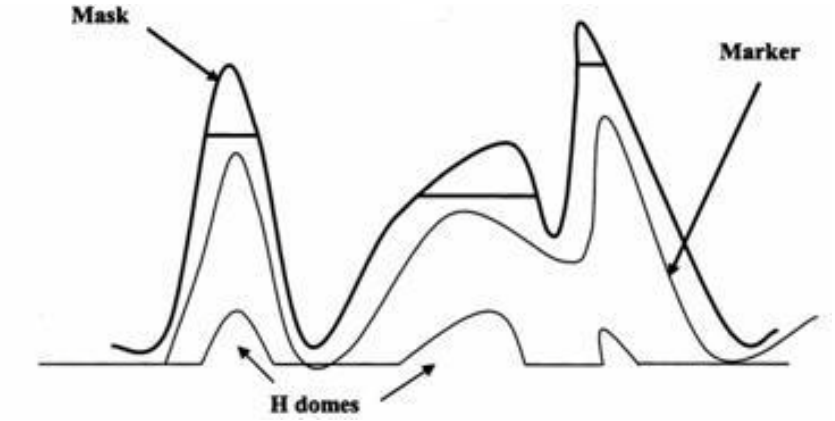

Fig. 13. H domes methodology. Tomado de [7].

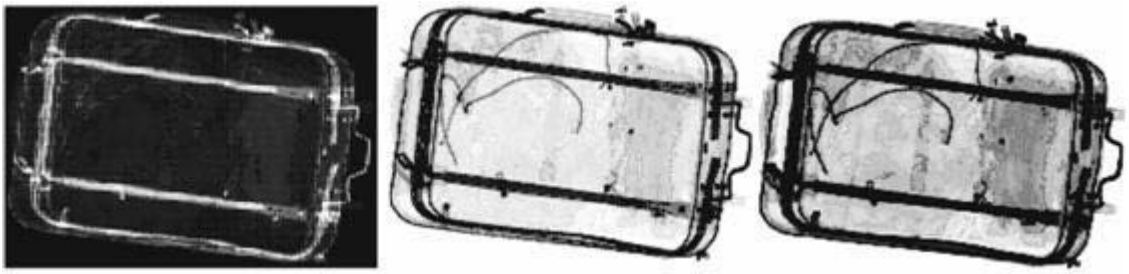

(a) **(b)** **(c)**

Fig. 14. (a) original image, (b) negative image, (c) result of H domes. Tomado de [7].

2.3 Pseudo-coloring

The main purpose of color-coding is enhancing the perceptual capabilities of the human visual system of airport screeners to extract more information from the image. The commercial systems in use like

Heimman 2004 and THScan introduce color schemes in x-ray luggage inspection. The atomic number of the material is determined using two images, one at low energy and the other at high energy, and color is assigned based on atomic number values. There was no published work describing the perceptual or cognitive basis on which this color combination was selected. Abidi et al. [8] described a series of linear and nonlinear pseudo-coloring maps designed and applied to single energy x-ray luggage scans to assist airport screeners in identifying and detecting threat items, particularly hard to see low-density weapons in luggage. They obtained significant increase up to 97% in the rate of threat detection, compared to results obtained from the original data.

2.3.1 RGB-Based Color Maps

The process is based on the analysis of the tri-stimulus value of the required output image by defining a function $P[\,]$, which maps the original grayscale data $I(x, y)$ to the primary color values $R(x,y), G(x,y)$, and $B(x,y)$.

$$I(x,y) \Rightarrow \begin{Bmatrix} P_R[\,] \\ P_G[\,] \\ P_B[\,] \end{Bmatrix} \Rightarrow \begin{matrix} R(x,y) \\ G(x,y) \\ B(x,y) \end{matrix} \Rightarrow C(x,y)$$

where $I(x,y)$ is original gray scale image and $C(x,y)$ is the pseudocolored image. Varying $P[\,]$several color-coded image can be obtained.

No Linear Mapping

This method obtains a new color scale as an extended version from a smaller color scale. For example in [7] a 256-step scale as can be seen in Figure 15 was developed and applied to x-ray luggage scans as an extended version to the 16-step color scale. The 16 original colors were utilized as base colors and intermediate colors computed by linearly interpolating the red, green, and blue intensity values from each base color to the next. The new color scale offers more details to discriminate objects.

The linear interpolation method can be understood as follows. Let R_i, G_i, $B_i$and R_{i+1},G_{i+1} ,B_{i+1} represent any two adjacent base colors; $I_i$and I_{i+1} denote their corresponding gray levels. Given a gray level I ($I_i < I_{i+1}\, for\, 1 \leq i \leq 15$), the associated intermediate color C = (R,G,B) between base colors C_i and C_{i+1} can be found using:

$$\boldsymbol{R = R_i + \left(R_{i+1} - R_i \left(\frac{I - I_i}{I_{i+1} - I_i} \right) \right)}$$

$$\boldsymbol{G = G_i + \left(G_{i+1} - G_i \left(\frac{I - I_i}{I_{i+1} - I_i} \right) \right)}$$

$$\boldsymbol{B = B_i + \left(B_{i+1} - B_i \left(\frac{I - I_i}{I_{i+1} - I_i} \right) \right)}$$

(a) (b)

Fig. 15. (a) 16-step scale and (b) 256-step scale obtained by non- lineal method.

Figure 16 shows the result after applying the no linear color mapping method.

Fig. 16. Original image *(left)* and colored version of original image after applied no linear color mapping *(right).*

Algebraic Transforms

In this method color is assigned through an algebraic formula applied to individual or group of pixels to create various combinations of the original pixels and obtain their color counterparts. Abidi et al. [8] described an example formula.

$$R = {}^{N}/_{L}$$

$$B = |\,{}^{2N}/_{L} - 1\,|$$

$$G = {}^{1-N}/_{L}$$

where L is the numbers of colors that can be supplied by the user and N is a number varying from 1 to L, where the grayscale was divided into L equal intervals corresponding to the L colors. Values belonging to the same interval will have the same single color. Varying the number of color different effects in the colored image, such as a variable amount of detail and clutter can be achieved. Figure 17 shows the result using this method to a color coded gray scale image and shows the different effects that can be obtained varying the number of colors L.

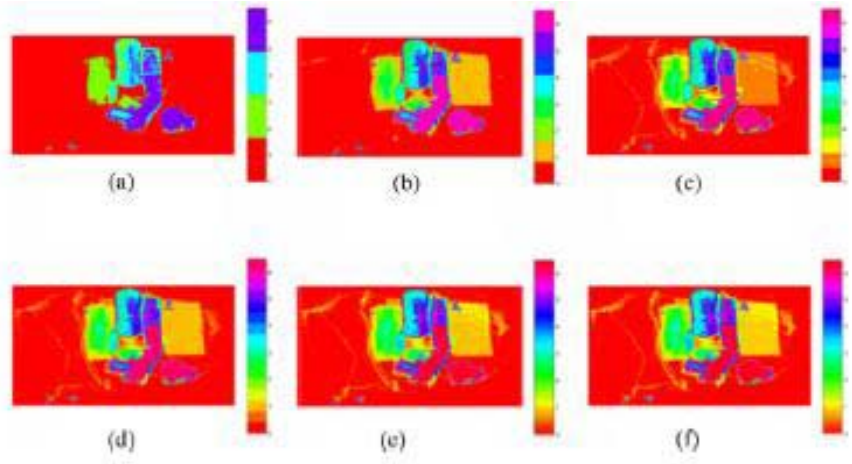

Fig. 17. Effects of varying the number of colors (a) 4 colors (b) 8 colors (c) 12 colors (d) 16 colors (e) 64 colors (f) 256 colors.

Trigonometric Transforms

Gonzalez and Woods [4] described an approach where three independent mathematical transforms were performed on the gray level data using sine functions.

$$R = |\sin(\omega_R I + \theta_R)|$$

$$G = |\sin(\omega_G I + \theta_G)|$$

$$B = |\sin(\omega_B I + \theta_B)|$$

where $\omega_R, \omega_G, \omega_B$ are the frequencies for the R,G, and B channels and $\theta_R, \theta_G, \theta_B$ are their corresponding phase angles. Changing the frequency and phase of each sine function would emphasize certain ranges of the grayscale.

Abidi et al. [8] described a particular case of sine transforms called rainbow transforms expressed by:

$$R = \left(1 + \cos\left(\frac{4\pi}{3 * 255} I\right)\right)\Big/_2$$

$$G = \left(1 + \cos\left(\frac{4\pi}{3 * 255} I - \frac{2\pi}{3}\right)\right)\Big/_2$$

$$B = \left(1 + \cos\left(\frac{4\pi}{3 * 255} I - \frac{4\pi}{3}\right)\right)\Big/_2$$

Figure 18 shows the result of applying a trigonometric transform described in (Besma Abidi Y. Z., 2006).

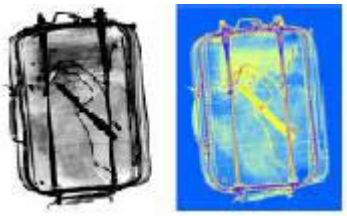

Fig. 18. Original image (l*eft)* and colored version after applying trigonometric transforms *(right).*

2.3.2 HSI-based color maps

Abidi et al. [7] described two classes of HSI-Based color transforms to improve low density objects detection. Color transforms in the first category provide a direct mapping between the gray values and their color counterparts, while color transforms in the second category were created by first performing a selected series of enhancements on the x-ray luggage scan to extract or emphasize features of interest, and then the results are fed into the H, S, and I components to create a composite chromatic image.

Mapping of Raw Grayscale Data

The process is based on the analysis of the tri-stimulus value of the required output image by defining a function *P* [], which maps the original gray values *G* to the HSI model components: hue, saturation and intensity. Abidi et al. [8] designed a color scale called ¨Springtime ¨, the hue and intensity; components of HSI model are given by the equations:

$$H = \frac{1}{2} - \frac{1}{2} * \sqrt{\left(1 - \left(\frac{G}{G_{max}}\right)^2\right)}$$

$$I = \ln\left(\frac{G+1}{G_{max}+1}\right)$$

where G is the gray value and G_{max} is the maximum gray value. The saturation component was set to constant equal 0.8.

Mapping of Preprocessed Data

These methods can be grouped in methods that use a constant saturation, and methods that use a data-dependent saturation [8].

Constant Saturation:

This procedure consists in feeding the hue and the intensity component of the HIS model with the result of several combination of image enhancement techniques while the saturation is a constant value. In [8] two color mappings called ¨"CS1" and "CS2 are described". The two maps are designed as follows:

"CS1"

$H = E_1$ = original + histogram equalization + contrast stretching, S = constant
$I = E_2$ = original + negative + H-domes [6] + contrast stretching

"CS2¨"

$H = E_1$' = original + negative, S = constant
$I = E_1$ = original + histogram equalization + contrast stretching

In both maps the saturation is a constant within the interval [0.6, 1].

Variable Saturation:

In this method E_1 is fed into both hue and saturation while E_2 is fed into intensity. Two color maps called "VS1" and "VS2" was described in [8].

"VS1"

$H=S=E_1$= original + histogram equalization + contrast stretching
$I= E_2$ = original + negative + H-domes + contrast stretching

"VS2"

$H=S=E_1$'= original + negative
$I= E_1$ = original +histogram equalization + contrast stretching

3 Dual Energy X-ray Image Fusion

The aim of dual energy x-ray image fusion is to integrate complementary information from the low energy x-ray image and the high-energy x-ray image such that the produced combined image is more amenable for a successful screeners' interpretation. The image obtained can be post-processed with the methods described in Chapter 2. In this chapter two image fusions are described. The first method proposed in [9] is based on local spatial information; the second method [10] is based on wavelet transform.

3.1 Image Fusion Using Local Spatial Information

The method consists in obtaining two images: background image and detail image and summing these images to obtain the fused image. Figure 19 describes how to obtain these images from low energy and high energy images.

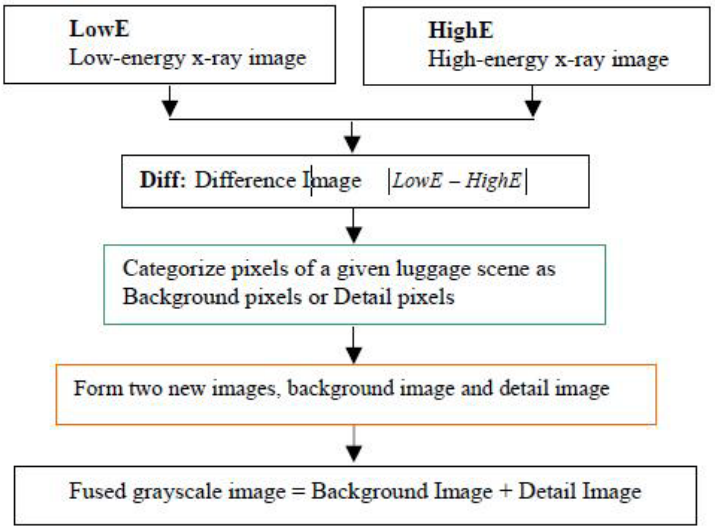

Fig. 19. Flow chart of Dual energy x-ray images fusion using local special information method.

To categorize the pixels in background pixel or detail pixel a threshold is required, if any pixel in the difference image is equal or less than the specified threshold, the pixel is classified as background pixel, else the pixel is categorized as detail pixel. To form the background and detail images the following rules are used:

$$Background\ Image = \begin{cases} (LowE + HighE)/2 & for\ background\ pixels \\ 0 & for\ details\ pixels \end{cases}$$

$$Detail\ Image = \begin{cases} LowE & if\ |R - HighE| < |R - LowE| \\ HighE & if |R - HighE| \geq |R - LowE| \\ 0 & for\ background\ pixels \end{cases} \quad for\ detail\ pixels$$

The fused image is processed finally for noise removal. To characterize the noise, the authors analyzed a small patch from an area of the image where pixel values should be constant. Observing the shapes of the histograms of the small patches taken from the same spatial location of each pair of low and high-energy images, they approximated the noise with a Gaussian function. To reduce the presence of noise, an adaptive and local noise-removal filter, Wiener filter [4], is applied to the fused image.

3.2 Wavelet-Based Image Fusion

Chen et al. [10] described a wavelet-based image fusion as fallow:

1. Each registered source image is transformed into corresponding wavelet coefficient images using the discrete wavelet transform (DWT) [13];
2. By following a fusion rule, the fused wavelet coefficients are computed from the corresponding wavelet coefficients of the source images;
3. The inverse DWT (IDWT) [13] is applied to the fused wavelet coefficients to reconstruct the fused image. Figure 20 depicts the wavelet-based image fusion method.

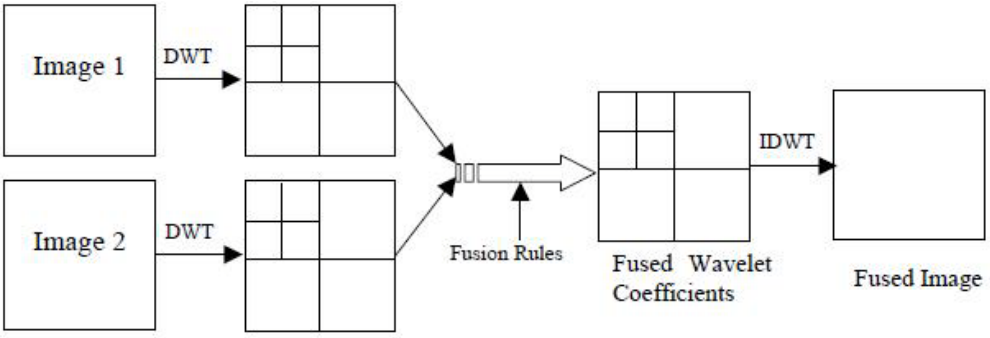

Fig. 20. Procedure of Dual energy x-ray images fusion using local Wavelet transform.

To obtain the wavelet coefficients of Low Energy (L) and High Energy (H) images a wavelet family and a wavelet basis capable of representing image details need to be selected. Another issue to be determined is how many scales are necessary for the decomposition. Few scales will cause the loss of too many details in the fused image, and many scales will result in a rough fused image which is difficult for screeners to interpret. The authors demonstrated that by using four scales in dual energy x-ray images generally we could yield good results [10]. They applied a low pass filter to the approximation coefficients of L and H respectively, to generate the approximation coefficients of the fused image .The approximation coefficients of the fused image is generated by averaging the approximation coefficients of L and H. To obtain the details coefficients of the fused image they combine the corresponding detail coefficients of L and H. The details coefficients are calculated at all decomposition scales of the fused image by summing the corresponding detail coefficients of L and H. The fused image is constructed by performing IDWT using the approximation coefficients and detail coefficients. Finally the fused image is noise removal by background noise subtraction.

4 Proposed Taxonomy

As we explained above the methods for processing x-ray luggage images can be clustered into two primary groups: those designed for a single conventional x-ray image and those using information of two images obtained at two different x-ray energy levels, for example dual energy x-ray systems. The methods of the first group can be subdivided into three groups, enhancement methods, declustering methods and pseudo-coloring methods. The pseudo-coloring methods published are based on RGB or HSI colors models. The methods for the fusion of two x-ray images can be subdivided into two groups: methods based on local spatial information and methods based on wavelet transform. Figure 21 depicts the new taxonomy that we proposed.

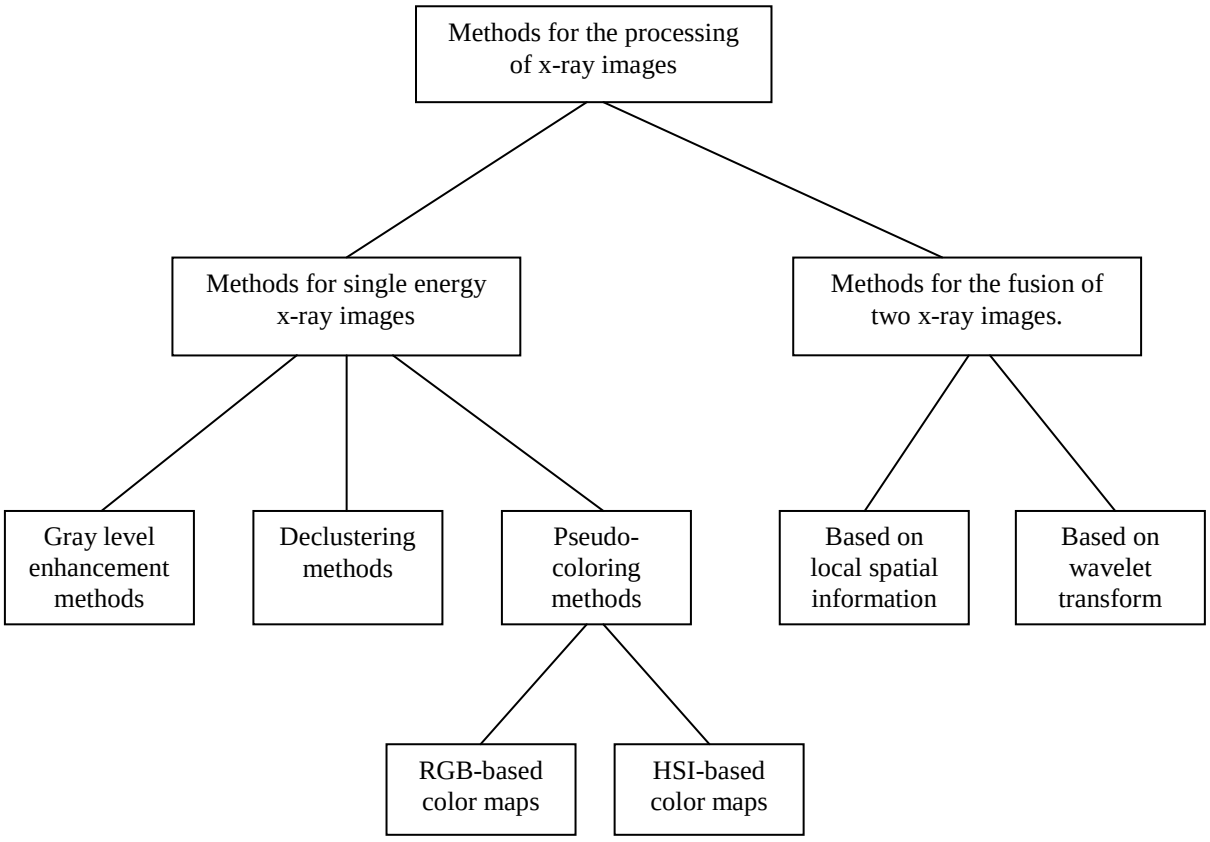

Fig. 21. Proposed taxonomy.

5 Conclusions

The recognition of threat objects in x-ray images for the airport security field is at an early stage. As conclusion of the study we can say that most of the works that have been published in the detection of threat objects in x-ray images of baggage are aimed at improving the visual quality of image for manual recognition by human experts. In this technical report several so-called “image enhancement” methods to help decision making by humans were described. These are traditional methods of image processing which have been designed for reflectance images without taking into account the physical principle of formation of x-ray image, which is based on capturing the transmittance of objects.

Although significant increases in detection rates using these techniques have been reported, we believe that the study of new and specific approaches for this kind of images are needed, for example methods that consider the transparency properties present in these images should be investigated.

References

1. Singh, S.: Explosives detection systems (EDS) for aviation security. Journal Signal Processing, Volume 83, Issue 1 (January 2003)
2. Hardmeier, D., Hofer, F. and Schwaninger, A.: The X-ray object recognition test (X-ray ORT) - a reliable and valid instrument for measuring visual abilities needed in X-ray screening. In: 39th Annual International Carnahan Conference on Security Technology, 2005 (CCST '05) 189 - 192

3. Michel, S., Koller, S., Ruh, M. and Schwaninger, A.: The effect of image enhancement functions on x-ray. In: Proceedings of the 4th International Aviation Security Technology Symposium, Washington, D.C., USA, (2006) 434-439
4. Gonzalez, R. and Woods, R.: Digital Image Processing (3rd Edition). Prentice-Hall, Inc. Upper Saddle River, NJ, USA (2006)
5. Nercessian, S., Panetta, K. and Agaian, S.: Automatic Detection of Potential Threat Objects in X-ray Luggage Scan Images. IEEE Conference on Technologies for Homeland Security (May 2008) 504-509
6. Abidi, B.R., Liang, J., Mitckes, M. and Abidi, M.: Improving the detection of low-density weapons in x-ray luggage scans using image enhancement and novel scene-decluttering techniques. J. Electronic Imaging (2004) 523-538
7. Abidi, B.R., Mitckes, M., Abidi, M., Liang, J.: Grayscale enhancement techniques of x-ray images of carry-on luggage. International conference on quality control by artificial vision, Volume 5132 (2003) 579-591
8. Abidi, B.R., Zheng, Y., Gribok, A.V., Abidi, M.: Improving Weapon Detection in Single Energy X-Ray Images Through Pseudocoloring. IEEE Transactions on Systems, Man, and Cybernetics, Part C: Applications and Reviews, Volume 36, Issue 6 (November 2006) 784 - 796
9. Zheng, Y.: X-Ray Image Processing and Visualization for Remote Assistance of Airport Luggage Screeners. MsC Thesis, The University of Tennessee, Knoxville (2004) Supervisor - Prof. Dr. Mongi Abidi.
10. Chen, Z., Zheng, Y., Abidi, B.R, Page, D., Abidi, M.: A Combinational Approach to the Fusion, De-noising and Enhancement of Dual-Energy X-Ray Luggage Images. In: Proceedings of the IEEE Computer Society Conference on Computer Vision and Pattern Recognition (CVPR'05), Volume 03 (2005)
11. Heitz, G., Chechik, G.: Object Separation in X-Ray Image Sets. In: Proceedings of the IEEE Computer Society Conference on Computer Vision and Pattern Recognition (CVPR 2010)
12. Silver, B., Agaian, S., Panetta, K.: Contrast Entropy Based Image Enhancement and Logarithmic Transform Coefficient Histogram Shifting", in Proceedings of IEEE International Conference on Acoustics, Speech, and Signal Processing (ICASSP '05), Volume 2 (2005) 633 – 636
13. Nunez, J., Otazu, X., Fors, O., Prades, A., Pala, V., Arbiol, R.: Multiresolution-based image fusion with additive wavelet decomposition. IEEE Transactions on Geoscience and Remote Sensing. Volume 37, No. 3 (1999) 1204 – 1211

RT_043, octubre 2011
Aprobado por el Consejo Científico CENATAV

Editor: Lic. Lucía González Bayona
Diseño de Portada: Di. Alejandro Pérez Abraham
RNPS No. 2142
ISSN 2072-6287
Indicaciones para los Autores:
Seguir la plantilla que aparece en www.cenatav.co.cu
C E N A T A V
7ma. No. 21812 e/218 y 222, Rpto. Siboney, Playa;
La Habana. Cuba. C.P. 12200
Impreso en Cuba